

# Thermal behavior and entanglement in Pb-Pb and p-p collisions

X. Feal, C. Pajares, and R.A. Vazquez

*Instituto Galego de Física de Altas Enerxías &*

*Departamento de Física de Partículas*

*Universidade de Santiago de Compostela, 15782 Santiago, SPAIN*

(Dated: September 17, 2021)

The thermalization of the particles produced in collisions of small size objects can be achieved by quantum entanglement of the partons of the initial state as it was analyzed recently in proton-proton collisions. We extend such study to Pb-Pb collisions and to different multiplicities of proton-proton collisions. We observe that, in all cases, the effective temperature is approximately proportional to the hard scale of the collision. We show that such relation between the thermalization temperature and the hard scale can be explained as a consequence of the clustering of the color sources. The fluctuations on the number of parton states decreases with multiplicity in Pb-Pb collisions as far as the width of the transverse momentum distributions decreases, contrary to the p-p case. We relate these fluctuations to the temperature time fluctuations by means of a Langevin equation for the white noise due to the quench of a hard parton collision.

## I. INTRODUCTION

The presence of an exponential shape in the transverse momentum distribution (TMD) of the produced particles in collisions of small size objects together with the approximate thermal abundances of the hadron yields constitutes an indicative sign of thermalization. This thermalization, however, can not be achieved under the usual mechanism, namely final state interactions in the form of several secondary collisions.

The emergence of this phenomenon has been recently studied [1–4], showing that thermalization can be obtained during the rapid quench induced by the collision due to the high degree of entanglement inside the partonic wave functions of the colliding protons. Thus, the effective temperature obtained from the TMD of the particles produced in the collision depends on the momentum transfer, that is, it constitutes an ultraviolet cut-off on the quan-

tum modes resolved by the collision. In diffractive processes with a rapidity gap, the entire wave function of the proton is involved and no entanglement entropy arises. Consequently, we expect no thermal radiation as it has been observed.

In this paper we further explore the relation between parton entanglement and thermalization by studying p-p and Pb-Pb collisions at different multiplicities. In the second case we expect an interplay between thermalization and final state interactions leading to some differences with p-p collisions concerning the entanglement and thermalization.

We show that the TMD of both collisions at different multiplicities can be fitted by the sum of an exponential plus a power like function, characterized by a thermal like temperature  $T_{\text{th}}$  and a temperature scale  $T_h$  respectively. For any fixed multiplicity and in all collisions the relation  $4T_{\text{th}} \approx T_h$  is satisfied. The power index  $n$  describing the hard spectrum behaves differently in p-p and in Pb-Pb collisions, showing the different behavior of the transverse momentum fluctuations. This behavior and the relation between  $T_{\text{th}}$  and  $T_h$  can be naturally explained in the clustering of color sources. The cluster size distribution of the clusters of overlapping strings found in the collision coincides with the distribution of temperatures obtained as solution of the Fokker-Planck equation associated to the linear Langevin equation for a white Gaussian noise produced by a fast quench in a hard parton collision.

The organization of the paper is as follows. In section II we introduce the entanglement of the partonic state following reference [1] and we analyze the TMD of p-p and Pb-Pb collisions at different multiplicities. In section III we discuss the obtained results remarking the similarities and differences of p-p and Pb-Pb collisions in connection with thermalization and entanglement. We briefly discuss the clustering of color sources in connection with the TMD in section IV and in the section V we introduce the Langevin and Fokker-Planck equations to study the time temperature fluctuations. Finally in section VI the conclusions are presented.

## II. ENTANGLEMENT, THERMALIZATION, AND TRANSVERSE MOMENTUM DISTRIBUTIONS

A hard process with momentum transfer  $Q$  probes only the region of space  $H$  of transverse size  $1/Q$ . Let us denote by  $S$  the region of space complementary of  $H$ . The proton is

described by the wave function

$$|\Psi_{HS}\rangle = \sum_n \alpha_n |\Psi_n^H\rangle |\Psi_n^S\rangle, \quad (1)$$

of a suitably chosen orthonormal sets of states  $|\Psi_n^H\rangle$  and  $|\Psi_n^S\rangle$  localized in the domains  $H$  and  $S$ . In the parton model this full orthonormal set of states is given by the Fock states with different number  $n$  of partons. The state (1) can not be separated into a product  $|\varphi^H\rangle \otimes |\varphi^S\rangle$  and therefore  $|\Psi_{HS}\rangle$  is entangled. The density matrix of the mixed state probed in region  $H$  is

$$S_H = \text{Tr}_S \rho_{SH} = \sum_n \langle \Psi_n^S | \Psi_{HS} \rangle \langle \Psi_{HS} | \Psi_n^S \rangle = \sum_n |\alpha_n|^2 |\Psi_n^H\rangle \langle \Psi_n^H|, \quad (2)$$

where  $|\alpha_n|^2 = p_n$  is the probability of having a state with  $n$  partons, independently of whether their interaction is hard or soft. The Von Neumann entropy of this state is given by

$$S = - \sum_n p_n \log p_n. \quad (3)$$

We can consider that a high momentum partonic configuration of the proton when the collision takes place undergoes a rapid quench due to the QCD interaction. The onset  $\tau$  of this hard interaction is given by the hardness scale  $Q$ ,  $\tau \sim 1/Q$ . Since  $\tau$  is small the quench creates a highly excited multi-particle state. The produced particles have thermal-like exponential spectrum with an effective temperature  $T \approx (2\pi\tau)^{-1} \approx Q/2\pi$ . Thus, the thermal spectrum can be originated due to the event horizon formed by the acceleration of the color field [5]-[8]. On the other hand, the comparison with LHC data on hadron multiplicity distributions [2] indicates that the produced Boltzmann entropy is close to the entanglement entropy of equation (3).

In reference [1], the thermal component of charged hadron transverse momentum distribution in p-p collisions at  $\sqrt{s} = 13$  TeV is parameterized as [9-11]

$$\frac{1}{N_{\text{ev}}} \frac{1}{2\pi p_t} \frac{d^2 N_{\text{ev}}}{d\eta dp_t} = A_{\text{th}} \exp\left(-m_t/T_{\text{th}}\right), \quad (4)$$

where  $T_{\text{th}}$  is the effective temperature and  $m_t = \sqrt{m^2 + p_t^2}$  is the transverse mass. The hard scattering, meanwhile, is parameterized as,

$$\frac{1}{N_{\text{ev}}} \frac{1}{2\pi p_t} \frac{d^2 N_{\text{ev}}}{d\eta dp_t} = A_{\text{h}} \frac{1}{\left(1 + \frac{m_t^2}{nT_{\text{h}}^2}\right)^n}, \quad (5)$$

where the temperature  $T_h$  and the index  $n$  are parameters determined from the fit to the experimental data. The value  $T_{th} = 0.17$  GeV was found [1], agreeing with the one expected from the extrapolation of the relation

$$T_{th} = 0.098 \left( \sqrt{\frac{s}{s_0}} \right)^{0.06} \text{ (GeV)}, \quad (6)$$

obtained at lower energies. Similarly the hard scale  $T_h$  is given by the relation

$$T_h = 0.409 \left( \sqrt{\frac{s}{s_0}} \right)^{0.06} \text{ (GeV)}. \quad (7)$$

At  $\sqrt{s} = 13$  TeV, the values found for the hard scale are  $T_h = 0.72$  GeV and  $n = 3.1$ . We notice that from Equations (6) and (7) one finds

$$\frac{T_h}{T_{th}} \approx 4.2, \quad (8)$$

independently of the energy. The ratio of the particular values obtained in the fit [1] are close to this values.

In order to study the dependence on the multiplicity of  $T_{th}$  and  $T_{rmh}$  we have used the transverse momentum distribution of  $K_S^0$  produced in p-p collisions at  $\sqrt{s} = 7$  TeV in the range up to  $p_t \leq 10$  GeV/c [13]. We use  $K_S^0$  instead of  $\pi$  or charged particles because we have not found published data covering a broad range of soft and hard regions at different multiplicities. In Figures (1), (2) and (3), we show the fit and the results for  $T_h$  and  $T_{th}$  respectively as a function of  $dN_{ch}/d\eta$ . We observe an increase of  $T_h$  and  $T_{th}$ . The values of  $T_{th}$  and  $T_h$  are in the range [0.18,0.28] and [0.8,1.15]. In Figure (3) the scaled curve  $4T_{th}$  is shown compared to  $T_h$ . We observe that the scaled  $4T_{th}$  curve lies on the obtained  $T_h$  values, therefore the relation between  $T_{th}$  and  $T_h$  (8) remains approximately valid not only for different energies but also for different centralities, pointing out to some physical reason behind. The obtained values for  $T_{th}$  and  $T_h$  are slightly higher than the values  $T_{th} = 0.17$  GeV and  $T_h = 0.74$  GeV of reference [1] due to the different sets of data, since in this analysis  $K_S^0$  are used instead of charged particles.

We have extended the study to Pb-Pb collisions at different multiplicities by fitting the ALICE collaboration TMD data for charged particles [12] at  $\sqrt{s} = 2.76$  TeV. In Figures (4), (5) and (6), we show the fit and the values obtained for  $T_{th}$  and  $T_h$  as a function of the multiplicity.  $T_{th}$  also increases with multiplicity and  $T_h$  follows the same relation  $T_h \approx 4T_{th}$  observed at p-p collisions. In Figure (7) we show the results of the fit for the power index

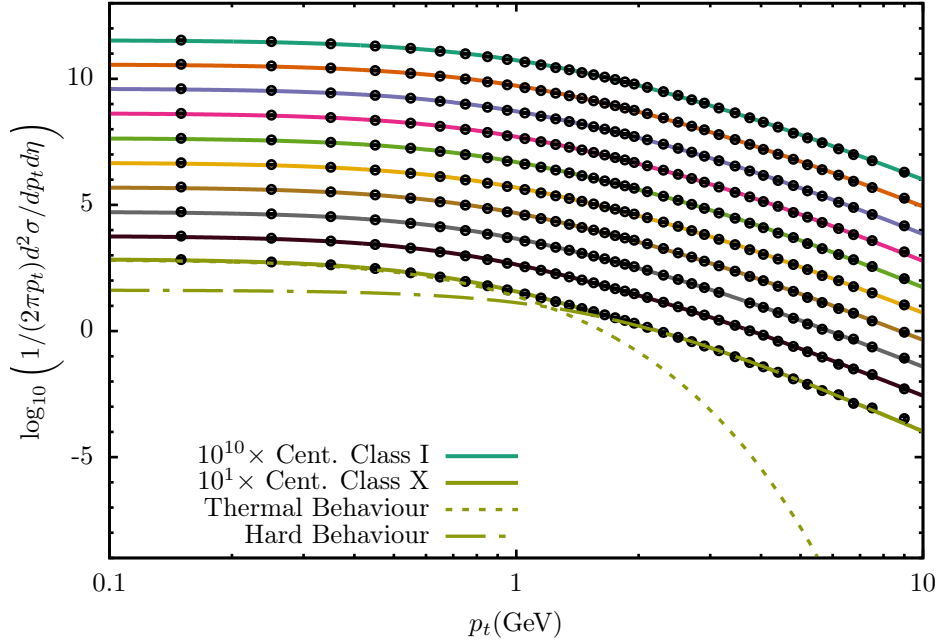


FIG. 1: Normalized differential  $K_S^0$  production in p-p collisions at  $\sqrt{s_{NN}} = 7$  TeV as a function of transverse momentum for different classes of centralities. Centrality classes from I to X, in decreasing magnitude, correspond to charged particle productions of  $dN_{ch}/d\eta = 21.3, 16.5, 13.5, 11.5, 10.1, 8.45, 6.72, 5.40, 3.90$  and  $2.26$ . Also shown are the thermal and hard components of the lowest centrality fit, by short dashed and long dashed lines, respectively.

$n$  in p-p and Pb-Pb collisions as a function of the charged particle production.  $n$  decreases with multiplicity for p-p collisions and, on the contrary, increases for Pb-Pb collisions. For p-p collisions at  $\sqrt{s} = 13$  TeV the value obtained for the case of charged particles is  $n = 3.1$ , slightly smaller than the value of Figure (7). The values of  $n$  are larger for Pb-Pb than for p-p collisions as expected due to the jet quenching and correspondingly to high  $p_t$  particle suppression.

### III. DISCUSSION

Our results for p-p collisions show that for each multiplicity the effective thermal temperature obtained from the TMD of the produced particles can be viewed as a rapid quench of the entangled partonic state. The behavior of  $T_{th}$  and  $T_h$  as a function of the multiplicity is very similar, holding the relation  $T_h \approx 4T_{th}$  for all the studied multiplicities. This fact adds

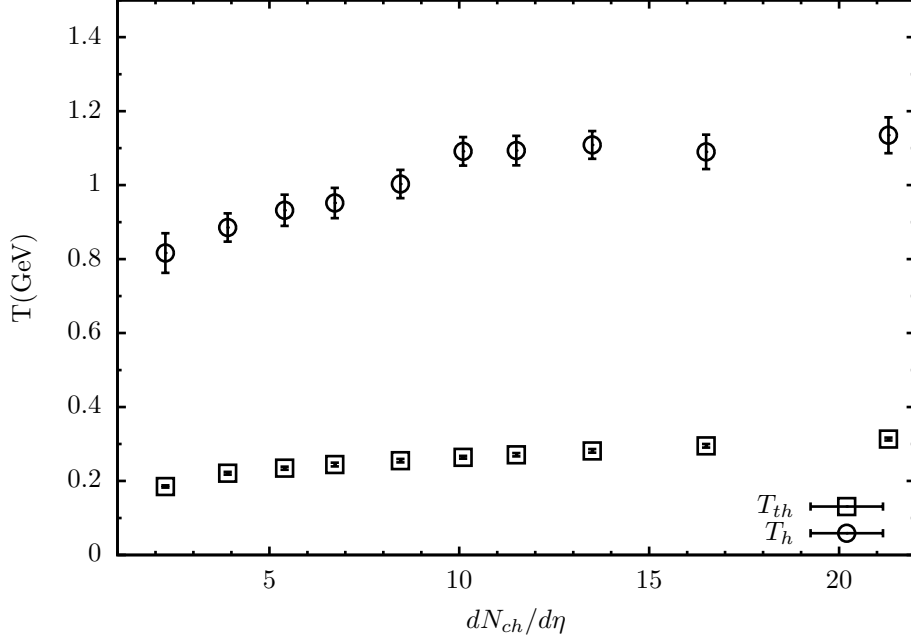


FIG. 2:  $T_{th}$  and  $T_h$  as a function of centrality for  $K_S^0$  production in p-p collisions at  $\sqrt{s_{NN}} = 7$  TeV.

evidence to the cases studied in reference [1]. It is remarkable that the same relation holds for Pb-Pb collisions, realizing the different values of  $T_{th}$  and  $T_h$  compared with the p-p case. The increase of  $T_{th}$  with multiplicity in p-p collisions is larger than in the Pb-Pb case as it was expected, as far as  $T_{th}$  is nothing but  $\langle p_t \rangle$  and experimentally the LHC data [12] has shown a larger increase with multiplicity in p-p than in Pb-Pb collisions.

Equations (4) and (5) can be obtained in the framework of clustering of color sources [14–16] as we show in section IV. In this approach,  $T_{th} \approx T_h/\pi\sqrt{2}$  and the cluster size distribution is a gamma function [17–20] which coincides with the stationary solution of the Fokker-Planck equation derived from the Langevin equation corresponding to a white noise due to the quench of a hard parton collision [21, 22]. In this way the fluctuation in the cluster size are related to the time temperature fluctuations.

The ratio  $R$  of the integral under the power law curve (hard component) and the integral over the total (hard + thermal components)

$$R = \frac{H}{H + S}, \quad (9)$$

is plotted in Figure (8), for different multiplicities for p-p and Pb-Pb collisions. The value found at  $\sqrt{s} = 13$  TeV in reference [1] was  $R \approx 0.16$ , in agreement with the ratio calculated

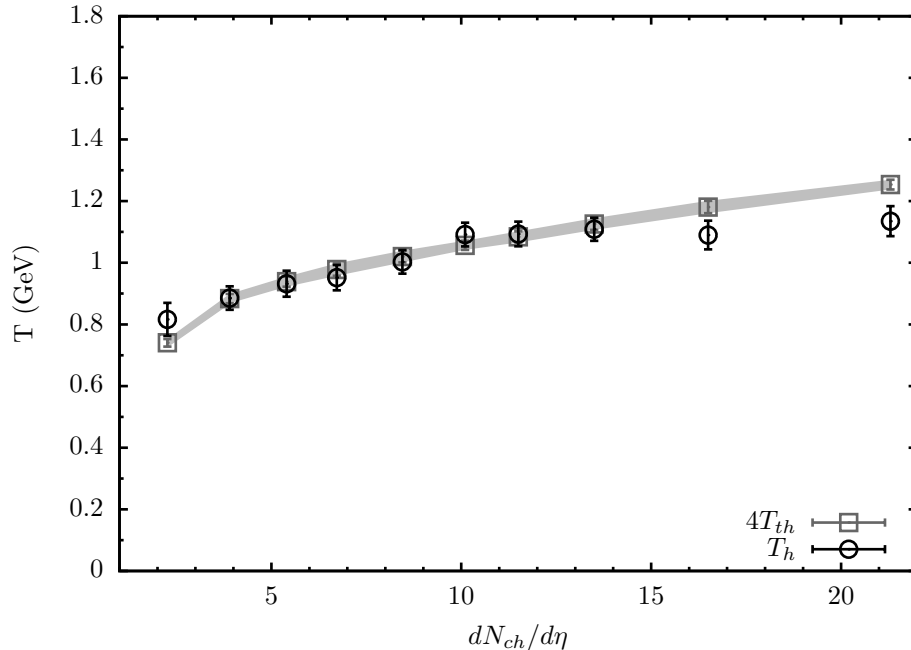


FIG. 3:  $T_h$  and  $4T_{th}$  as a function of centrality for  $K_S^0$  production in p-p collisions at  $\sqrt{s_{NN}} = 7$  TeV.

in inelastic proton-proton collisions at  $\sqrt{s} = 23, 31, 45$ , and  $53$  GeV. Our results for p-p collisions at  $\sqrt{s} = 7$  TeV for different multiplicities are close to the mentioned value. In the case of Pb-Pb we have found a smaller value. This smallness is consistent with the behavior found in [23] based on saturation momentum and geometrical scaling.

#### IV. CLUSTERING OF COLOR SOURCES

Multiparticle production is currently described in terms of color sources (strings) stretched between the projectile and the target. These strings decay by the Schwinger  $q\bar{q}$  production and subsequently hadronize to produce the observed hadrons. The color in the strings is confined in a small area in the transverse space of the order of  $0.2$  fm. With increasing energy and/or atomic number of the colliding objects, the number of color sources grows, and they start to overlap, forming clusters. A cluster of  $n$  color sources behaves as a single string with an energy-momentum that corresponds to the sum of the energy-momentum of the overlapping strings and with a higher color field, corresponding to the vectorial sum of the color charges of each individual string. The resulting color field covers

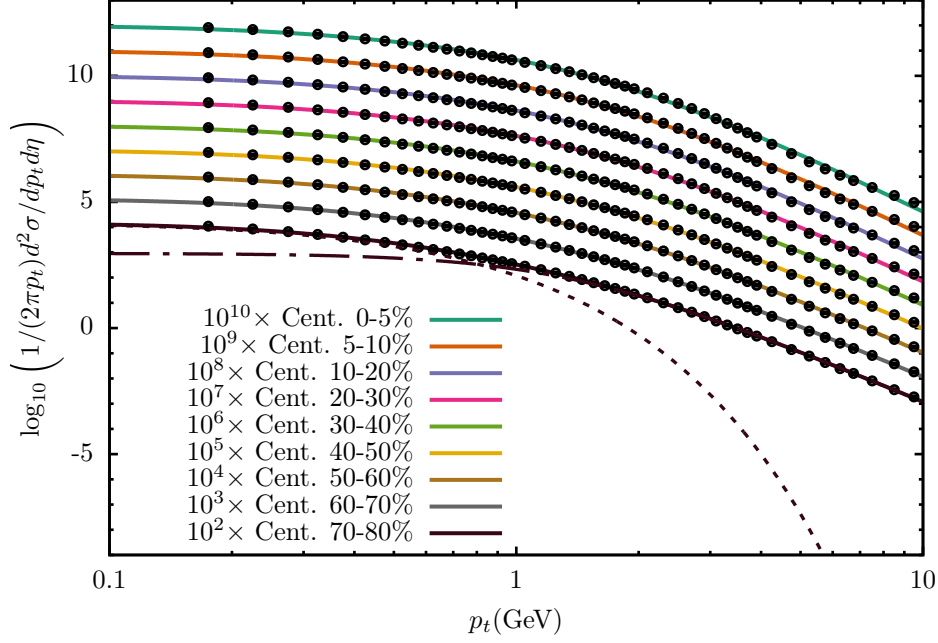


FIG. 4: Normalized differential charged particle production in Pb-Pb collisions at  $\sqrt{s_{NN}}=2.76$  TeV, as a function of transverse momentum for different classes of centralities. Centrality classes from 0%-5% to 70%-80%, in decreasing magnitude, correspond to charged particle productions of  $dN_{ch}/d\eta = 1600, 1290, 960, 650, 425, 260, 145, 75$  and  $30$ . Also shown are the thermal and hard components of the lowest centrality fit, by short dashed and long dashed lines, respectively.

the area  $S_n$  of the cluster. Thus  $\vec{Q}_n^2 = (\sum_1^n \vec{Q}_i)^2$ , and given that the individual string colors can be arbitrarily oriented in color space, the average  $\vec{Q}_i \cdot \vec{Q}_j$  is zero, so  $\vec{Q}_n^2 = n\vec{Q}_1^2$ . As  $Q_n$  depends also on the area, we have  $Q_n = \sqrt{nS_n/S_1}Q_1$ , where  $S_1$  is the area of the individual string. The mean multiplicity and the mean transverse momentum are proportional to the color charge and to the color field respectively

$$\mu_n = \sqrt{\frac{nS_n}{S_1}}\mu_1 \quad \langle p_t^2 \rangle_n = \sqrt{\frac{nS_1}{S_n}}\langle p_t^2 \rangle_1, \quad (10)$$

which in the limit of high density,  $\xi = N_s S_1/S$ , becomes

$$\mu_n = N_s F(\xi)\mu_1 \quad \langle p_t^2 \rangle_n = \frac{1}{F(\xi)}\langle p_t^2 \rangle_1, \quad (11)$$

where  $N_s$  is the number of color sources and  $F(\xi)$  is an universal factor

$$F(\xi) = \sqrt{\frac{1 - e^{-\xi}}{\xi}}. \quad (12)$$



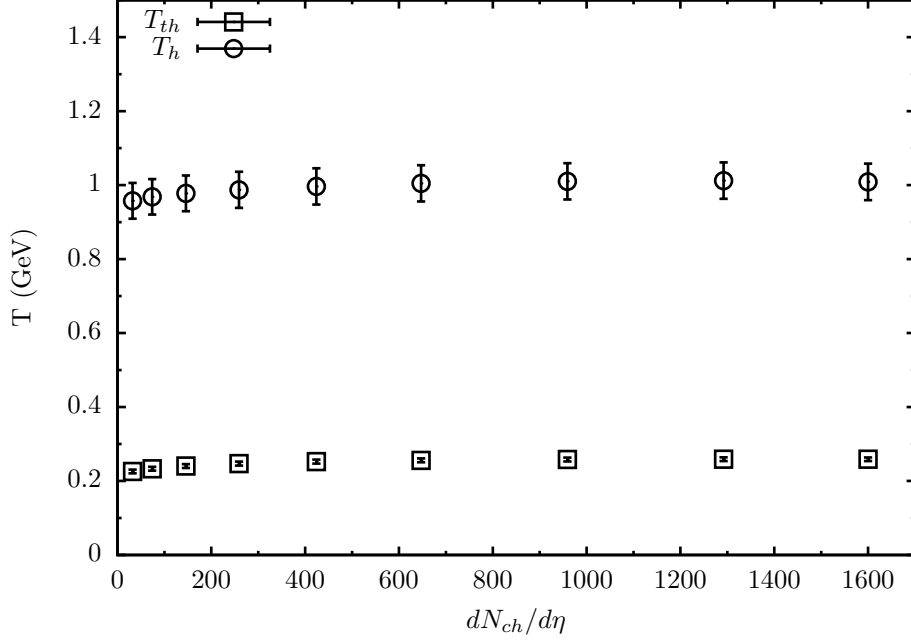


FIG. 5: Variation of  $T_{th}$  and  $T_h$  with centrality for charged particle production in Pb-Pb collisions at  $\sqrt{s} = 2.76$  TeV.

The factor  $1 - e^{-\xi}$  is the fraction of the total collision area covered by color sources at density  $\xi$  (it is assumed an homogeneous profile for the collision area).  $F(\xi)$  goes to 1 at low densities and goes to 0 at high  $\xi$ . The transverse momentum distribution  $f(p_t)$  is obtained from the Schwinger's distribution,  $\exp(-p_t^2 x)$ , weighted by the cluster size distribution  $W(x)$ , where  $x$  is the inverse of  $\langle p_t^2 \rangle_n$

$$f(p_t) = \int dx W(x) \exp(-p_t^2 x). \quad (13)$$

The weight function is the gamma function because the process of increasing the centrality or energy of the collision can be regarded as a transformation of the color field located in the sites of the surface area, implying a transformation of the cluster size distribution of the type

$$W(x') \rightarrow \frac{x'W(x')}{\langle x' \rangle} \rightarrow \dots \frac{x'^k W(x')}{\langle x'^k \rangle} \rightarrow \dots \quad (14)$$

This renormalization group type of transformation have been studied long time ago in probability theory showing that the only stable distributions under such transformations are the generalized gamma function. We take the simplest case, namely, the gamma function

$$W(x) = \frac{\gamma}{\Gamma(n)} (\gamma x)^n \exp(-\gamma x), \quad (15)$$

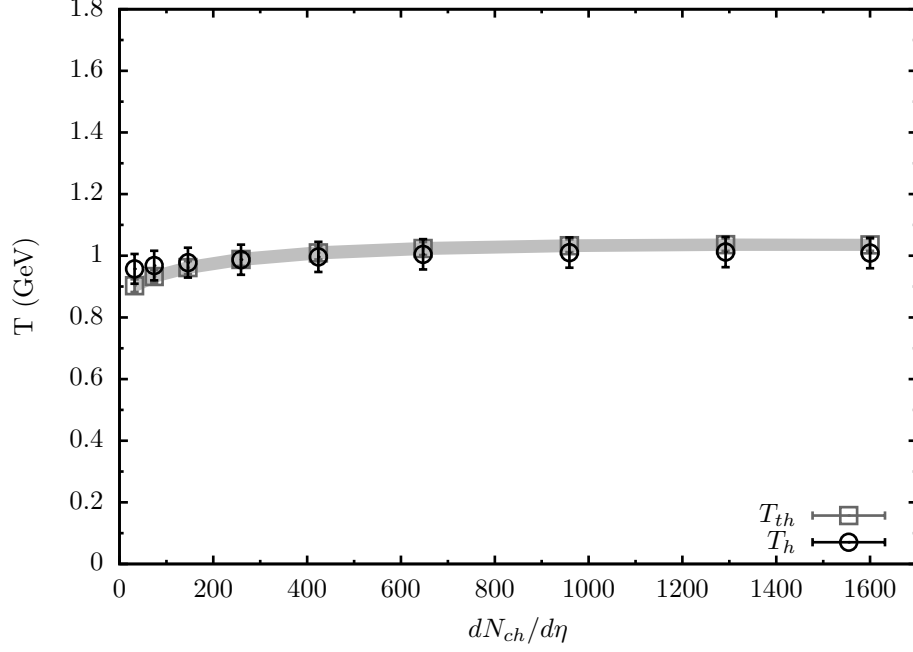


FIG. 6:  $T_h$  and  $4T_{th}$  as a function of centrality, for charged particle production in Pb-Pb collisions at  $\sqrt{s} = 2.76$  TeV.

with

$$\gamma = \frac{n}{\langle x \rangle}, \quad (16)$$

and

$$\frac{1}{n} = \frac{\langle x^2 \rangle - \langle x \rangle^2}{\langle x \rangle^2}. \quad (17)$$

Introducing eq. 15 into equation 13 we obtain the distribution [17]

$$f(p_t) = \frac{1}{(1 + p_t^2/\gamma)^n} = \frac{1}{(1 + \frac{F(\xi)p_t^2}{n\langle p_t^2 \rangle_1})^n}, \quad (18)$$

which takes the form of the parameterization used in the eq. 5 with

$$T_h^2 = \frac{\langle p_t^2 \rangle_1}{F(\xi)}, \quad (19)$$

which grows with the density  $\xi$  and thus with the energy and centrality as it is observed in the analysis of p-p and Pb-Pb collisions. In the last case, if the fits include larger  $p_t$  values it is observed a flattening of the dependence of  $T_h$  with multiplicity due to jet quenching effects. At low  $p_t$ , equation 18 behaves as

$$f(p_t) \approx \exp(-p_t^2 F(\xi)/\langle p_t^2 \rangle_1), \quad (20)$$

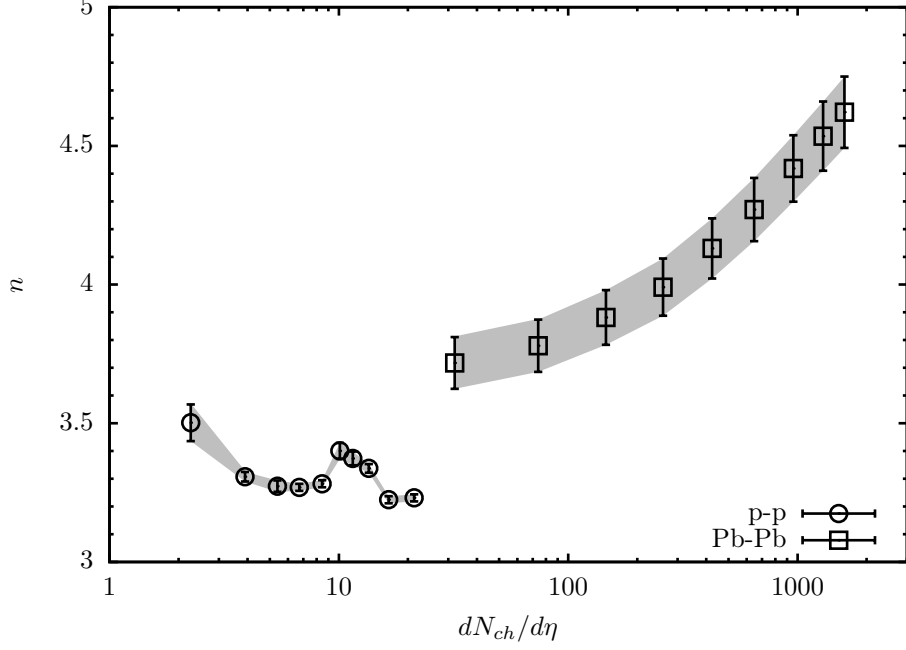


FIG. 7: Power index  $n$  of the hard component as a function of  $dN_{\text{ch}}/d\eta$  for  $K_S^0$  production in p-p at  $\sqrt{s} = 7$  TeV, and charged particle production in Pb-Pb collisions at  $\sqrt{s_{NN}} = 2.76$  TeV.

independently of  $n$ . In this low  $p_t$  regime, there are other effects, like fluctuations of the color field, which should be taken into account. In fact, assuming that such fluctuations are Gaussian, we have [6, 7]

$$\sqrt{\frac{2}{\pi \langle x_h^2 \rangle}} \int_0^\infty \exp\left(-\frac{x_h^2}{2 \langle x_h^2 \rangle}\right) \exp\left(-\frac{\pi p_t^2}{2 x_h^2}\right) = \exp\left(-p_t \sqrt{\frac{2\pi}{\langle x_h^2 \rangle}}\right) \quad (21)$$

where we defined  $x_h^2 = \pi T_h^2$ . The equation 21 expresses the thermal behavior with

$$T_{\text{th}} = \frac{T_h}{\pi \sqrt{2}}. \quad (22)$$

In other words, the thermal temperature is given by the fluctuations of the hard temperature which are proportional to this hard temperature.

We notice that according to equation 18 the power index  $n$  is related to the inverse of the width of the distribution and a different behavior with multiplicity is obtained for p-p and Pb-Pb collisions. This fact is a consequence of the clustering of the color sources. At low density of sources, there are only a few clusters of overlapping strings and thus the only temperature fluctuations come from inside the individual strings. As the number of clusters with different number of color sources increases, the fluctuations also increase and

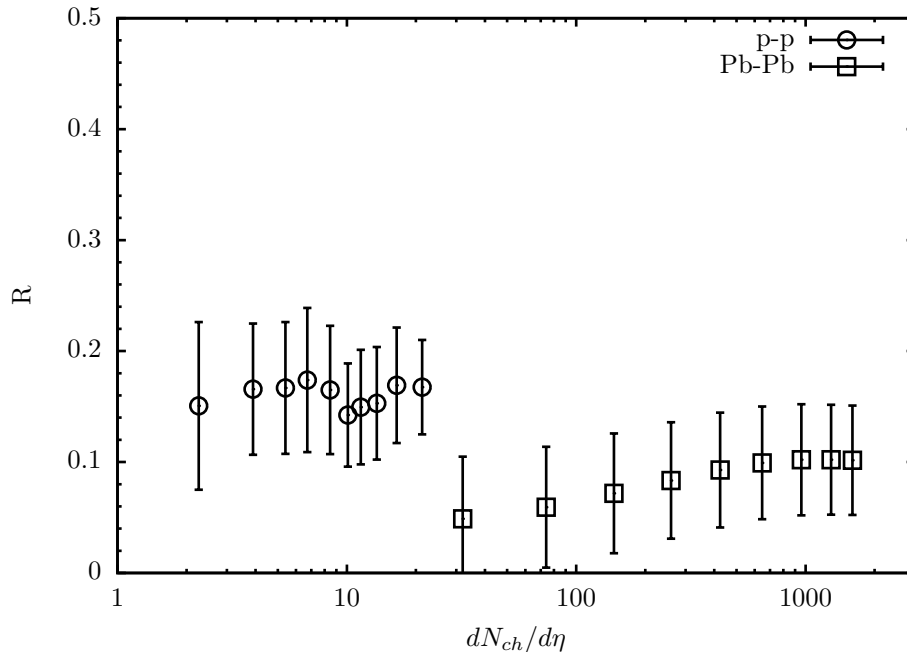


FIG. 8:  $R$ , the ratio of the hard component to the total component as a function of  $dN_{ch}/d\eta$ , for  $K_S^0$  production in p-p at  $\sqrt{s}=7$  TeV and for charged particle production in Pb-Pb collisions at  $\sqrt{s_{NN}}=2.76$  TeV.

correspondingly  $n$  decreases. If the color density increases further, the clusters of different color start to overlap in such a way that the number of clusters with different number of color sources decreases and thus the fluctuations decrease and  $n$  increases. The change of behavior which can be observed in fig. 7 is related to the critical percolation point. Notice that  $n$  is decreasing with multiplicity in p-p collisions but we expect that above a given multiplicity  $n$  should start to grow in the same way as in Pb-Pb collisions.

## V. TIME EVOLUTION

The scale of the TMD is  $u = T_h^2$  which obeys the Langevin equation

$$\frac{du}{dt} + \left( \frac{1}{\tau} + \zeta(t) \right) u = \phi, \quad (23)$$

where  $\tau$  is a characteristic damping time and  $\zeta(t)$  is a white Gaussian noise, with mean  $\langle \zeta(t) \rangle = 0$  and a correlator corresponding to fast changes such as expected in the quench

induced by a hard collision,

$$\langle \zeta(t)\zeta(t + \Delta t) \rangle = 2D\delta(\Delta t), \quad (24)$$

where  $D$  is the variance and  $\phi$  a constant.

The associated Fokker Planck equation for the probability to have the temperature  $T$  at time  $t$  under the above noise is given by [21, 22]

$$\frac{\partial f(T, t)}{\partial t} = -\frac{\partial}{\partial T} K_1 f(T, t) + \frac{1}{2} \frac{\partial^2}{\partial T^2} K_2 f(T, t), \quad (25)$$

being

$$K_1(T) = \phi - 2\frac{T^2}{\tau} + DT^2, \quad K_2(T) = 2DT^4.$$

The stationary solution of equations (23,25) is just the gamma distribution on the variable  $1/T^2$

$$f(T) = \frac{\mu}{\Gamma(n)} \left( \frac{\mu}{T^2} \right)^n \exp(-\mu/T^2), \quad (26)$$

with

$$\mu = \phi/D, \quad n = 1/\tau D. \quad (27)$$

This distribution coincides with the cluster size distribution of equation 15. In this way, the temperature fluctuations given by the inverse of the index  $n$  are related to the product  $\tau D$  which have to do with the time evolution.

## VI. CONCLUSIONS

The analysis of the dependence on the multiplicity of the LHC p-p and Pb-Pb data confirms the picture of thermalization induced by quantum entanglement. In all the analyzed data, the effective thermalization temperature obtained from data is proportional to the hard scale of the collision  $T$  given by the average momentum transfer. The coefficient of proportionality is universal, independent of the considered collision, even though  $T_{\text{th}}$  and  $T_{\text{h}}$  are different in each collision type. Thermal and hard temperatures increase with multiplicity in both collision scenarios, and this rise reproduces the known correlation of  $\langle p_t \rangle$  and  $dN_{ch}/d\eta$  for p-p and Pb-Pb collisions. In the framework of clustering of color sources the proportionality between  $T_{\text{th}}$  and  $T_{\text{h}}$  is understood, being  $T_{\text{th}}/T_{\text{h}} = \pi\sqrt{2}$ . The  $n$  parameter of the hard distribution decreases with multiplicity for  $p-p$  collisions and increases for Pb-Pb

collisions. This fact means that the normalized transverse momentum fluctuations behave quite different with multiplicity in p-p and Pb-Pb collisions. This behavior is naturally explained by the clustering of color sources. The change in the behavior of  $n$  is related to the formation of a large cluster of the initial color sources (partons), which marks the percolation phase transition.

The cluster size distribution is a gamma function which is also the stationary solution of the Fokker-Planck equation associated to the Langevin equation for a white Gaussian noise due to the quench of a hard partonic collision.

## VII. ACKNOWLEDGMENTS

We thank the grant María de Maeztu Unit of Excellence of Spain and the support of Xunta de Galicia under the project ED431C2017. This paper has been partially done under the project FPA2014-58293-C2-1-P of MINECO (Spain).

- 
- [1] O.K. Baker and D.E. Kharzeev, *Thermal radiation and entanglement in proton-proton collisions at the LHC*, arXiv:1712.04558.
  - [2] D.E. Kharzeev and E.M. Levin, *Deep inelastic scattering as a probe of entanglement*, Phys. Rev. D95 11 (2017) 114008.
  - [3] J.Bergers, S. Floerchinger, R. Venugopalan, *Dynamics of entanglement in expanding quantum fields*, JHEP 1804 (2018) 145.
  - [4] J.Bergers, S. Floerchinger, R. Venugopalan, *Thermal excitation spectrum from entanglement in an expanding quantum string*, Phys. Lett. B 778 (2018) 442.
  - [5] D.E. Kharzeev and K. Tuchin, *From Color Glass Condensate to Quark Gluon Plasma through the event horizon*, Nucl. Phys. A753 (2005) 316.
  - [6] J. Dias de Deus and C. Pajares, *Percolation of color sources and critical temperature*, Phys. Lett. B642 (2006) 455.
  - [7] P. Castorina, D. Kharzeev and H. Satz, *Thermal hadronization and Hawking-Unruh radiation in QCD*, Eur. Phys. J. C52 (2007) 187.

- [8] D.E. Kharzeev, E. Levin and K.Tuchin, *Multi-particle Production and Thermalization in High-Energy QCD*, Phys. Rev. C75 (2007) 044903.
- [9] A.A. Bylinkin and A.A. Rostovtsev, *Role of quarks in hadroproduction in high energy collisions*, Nucl. Phys. B888 (2014) 65.
- [10] A.A. Bylinkin, M.G. Ryskin and A.A. Rostovtsev, *Charged hadron distributions in a two component model*, Nucl. and Part. Proc. 273-275 (2016) 2746.
- [11] A.A. Bylinkin, D.E. Kharzeev and A.A. Rostovtsev, *The origin of thermal component in the transverse momentum spectra in high energy hadronic processes*, Int. J. Mod. Phys. E23 (2014) 1450083.
- [12] ALICE Collaboration, *Multiplicity dependence of the average transverse momentum in pp, p-Pb, and Pb-Pb collisions at the LHC*, Phys. Lett. B 727 (2013) 371.
- [13] ALICE Collaboration, *Enhanced production of multi-strange hadrons in high-multiplicity proton-proton collisions*, Nat. Phys. 13 (2017) 535.
- [14] M.A. Braun *et al.*, *De-Confinement and Clustering of Color Sources in Nuclear Collisions*, Phys. Rep. 599 (2015) 1.
- [15] N. Armesto, M.A. Braun, E.G. Ferreira and C. Pajares, *Percolation Approach to Quark-Gluon Plasma and  $J/\Psi$  Suppression*, Phys. Rev. Lett. 77 (1996) 3736.
- [16] M. Nardi and H. Satz, *String Clustering and  $J/\Psi$  Suppression in Nuclear Collisions*, Phys. Lett. B442 (1998) 14.
- [17] J. Dias de Deus, E.G. Ferreira, C. Pajares and R. Ugoccioni, *Universality of the transverse momentum distributions in the framework of percolation of strings*, Eur. Phys. J. C40 (2005) 229.
- [18] J. Dias de Deus, E.G. Ferreira, C. Pajares and R. Ugoccioni, *Schwinger Model and String Percolation in Hadron-Hadron and Heavy Ion Collisions*, Phys.Lett. B581 (2004) 156.
- [19] M.A. Braun and C. Pajares, *Implication of percolation of color strings on multiplicities, correlations and the transverse momentum*, Eur. Phys. J. C16 (2000) 349.
- [20] M.A. Braun and C. Pajares, *Transverse Momentum Distributions and Their Forward-Backward Correlations in the Percolating Color String Approach*, Phys. Rev. Lett. 85 (2000) 4864.
- [21] G. Wilk and Z. Wlodarczyk, *Interpretation of the nonextensivity parameter  $q$  in some applications of Tsallis statistics and Lévy distributions*, Phys. Rev. Lett. 84 (2000) 2770.

- [22] T.S. Biro and A. Jakovac, *Power-law tails from multiplicative noise*, Phys. Rev. Lett. 94 (2005) 132302.
- [23] C. Andres, A. Moscoso, and C. Pajares, *Universal geometrical scaling for hadronic interactions*, Nucl. Phys. A 901 (2013) 14.